JOURNAL OF AGRICULTURAL AND FOOD CHEMISTRY

# Induction of Autophagy and Apoptosis by the Extract of *Solanum nigrum* Linn in HepG2 Cells

HUI-MEI LIN,[†] HSIEN-CHUN TSENG,[†,‡] CHAU-JONG WANG,[†] CHARNG-CHERNG CHYAU,[||] KO-KAUNG LIAO,[§] PEI-LING PENG,[†] AND FEN-PI CHOU*,[†]

Institute of Biochemistry and Biotechnology, College of Medicine, and Department of Anatomy, Chung Shan Medical University, Department of Radiation Oncology, Chung Shan Medical University Hospital, and Research Institute of Biotechnology, Hungkuang University, Taichung 402, Taiwan

*Solanum nigrum* L. (SN) has been used in traditional folk medicine to treat different cancers. It is also used as a hepatoprotective and anti-inflammatory agent. In this study, we demonstrated that the extract of SN (SNE) induced a strong cytotoxic effect toward HepG2 cells but much less to Chang liver and WRL-68 cells. The mechanisms of the cytotoxic effect were concentration-dependent. High doses of SNE (2 and 5 mg/mL) induced apoptotic cell death in HepG2 cells, as evidenced by increases in the expressions of p-JNK and Bax, mitochodrial release of cytochrome *c*, and caspase activation. On the other hand, cells treated with low concentrations of SNE (50−1000 $\mu$g/mL) revealed morphological and ultrastructural changes of autophagocytic death under electron microscopic observation. Furthermore, these cells showed increased levels of autophagic vacuoles and LC3-I and LC3-II proteins, specific markers of autophagy. The levels of Bcl-2 and Akt that have been implicated in the down-regulation of autophagy were decreased upon SNE treatment. Taken together, these findings indicate that SNE induced cell death in hepatoma cells via two distinct antineoplastic activities of SNE, the ability to induce apoptosis and autophagocytosis, therefore suggesting that it may provide leverage to treat liver cancer.

**KEYWORDS:** ***Solanum Nigrum* Linn; apoptosis; autophagy; acidic vesicular organelle; antineoplastic activity**

## INTRODUCTION

Hepatocellular carcinoma (HCC) is a deadly disease with poor prognosis and a 5 year survival rate of about 5%. It is one of the most common human malignancies in sub-Saharan Africa, South East Asia, and China. Although the incidence of HCC is generally lower in developed countries such as the United States, France, the United Kingdom, and Japan, it has increased significantly over the past decade (*1*). According to World Health Organization statistics, of 6350000 cancer cases reported each year, 4% are HCC, 42% of which occur in China. Traditional treatment of liver tumors typically has been surgical resection and chemotherapeutics. However, these commonly used techniques are frequently challenged in view of metastasis and other pathological changes. Therefore, the development of new agents for hepatocellular cancer is important to reduce the mortality caused by this disease.

*Solanum nigrum* L. (SN) is an herbal plant indigenous to Asia and grows wildly and abundantly in open fields. It has been used in traditional Oriental medicines for treating various kinds of tumors and is believed to have various biological activities (*2*). For examples, SN has been used to cure hepatic cancer for a long time in Oriental medicine (*3*). Previous investigations have shown that extracts of SN suppressed the oxidant-mediated DNA−sugar damage (*3*), and the plant exerted cytoprotection against gentamicin-induced toxicity on Vero cells (*4*) and antineoplastic activity against Sarcoma 180 in mice (*5*). More recent studies revealed that extracts of SN induced apoptosis in MCF-7 cells (*2*) and inhibited 12-*O*-tetradecanoylphorbol-13-acetate-induced tumor promotion in HCT-116 cells (*6*). The ethanol extract of dried fruits of SN had a remarkable hepatoprotective effect in $CCl_4$-induced liver damage (*7*). These studies suggest that SN possesses a beneficial activity as an antioxidant and antitumor-promoting agent, although the mechanism for the activity remains to be elucidated.

In Chinese traditional medicine, SN is believed to have antitumor properties against many types of cancer, including liver cancer, breast cancer, lung cancer, stomach cancer, colon cancer, and bladder cancer, and is also used as a hepatoprotective and anti-inflammatory agent, although the mechanism for the

* To whom correspondence should be addressed. Tel: +886-4-24730022 ext. 11676. Fax: +886-4-23248195. E-mail: fpchou@csmu.edu.tw.
‡ Department of Radiation Oncology, Chung Shan Medical University Hospital.
† Institute of Biochemistry and Biotechnology, College of Medicine, Chung Shan Medical University.
§ Department of Anatomy, Chung Shan Medical University.
|| Research Institute of Biotechnology, Hungkuang University.

10.1021/jf062406m CCC: $37.00 
Published on Web 04/10/2007

activity remains to be elucidated (*3*, *4*). The latest report revealed that the ethanol extract of dried fruits of SN has a remarkable hepatoprotective effect against $CCl_4$-induced liver damage (*7*). This study developed some understanding of the effects of SN on liver cancer cells to evaluate its therapeutic application in treating liver cancer.

SN has been reported to contain many polyphenolic compounds, mainly flavonoids and steroids. The antioxidant and antitumor activity of SN may be due to the presence of polyphenolic constituents. The presence of steroidal glycosides, steroidal alkaroids, steroidal oligoglycosides, solamargine, and solasonine has also been detected (*8*).

The purpose of this work was to study the effects of SN on liver cancer cells to evaluate its therapeutic potential in treating liver cancer. In this report, we describe experiments that showed that water extracts of SN induced programmed cell death in liver cancer cells. The death mechanism was characterized, revealing that SN not only initiated apoptosis but also caused cell death through autophagocytosis (type II programmed cell death). The results of this investigation provide scientific evidence for the application of this herbal medicine in liver cancer therapy.

## MATERIALS AND METHODS

**Preparation of Extracts of SN (SNE).** The whole plant of SN was collected from the mountain in Miaoli, Taiwan. The plants were washed, cut into small pieces, shade-dried for 3 days, and then dried overnight in an oven. The dried SN (800 g) was mixed with water (5000 mL) for 30 min and subjected to continuous hot extraction (100 °C, 40 min). The resulting water extract was filtered and subsequently concentrated with a water bath (90 °C) until it became creamy and was dried in an oven (70 °C) that finally gave 185 g (23.125% of initial amount) of powder (water extract of SN). The concentration used in the experiment was based on the dry weight of the extract.

**Determination of Total Phenolics, Polysaccharide, and Protein.** The concentration of total phenols was analyzed according to the Folin−Ciocalteu method (*9*). Briefly, SNE (0.1 mg) was dissolved in a test tube with 1 mL of distilled water, and Folin−Ciocalteu reagent (2 N, 0.5 mL) was then added and mixed thoroughly. After an interval of 3 min, 3 mL of 2% $Na_2CO_3$ solution was added, and the mixture was allowed to stand for 15 min with intermittent mixing. The absorbance of the mixture at 750 nm was measured on a Hitachi U-3210 spectrophotometer (Hitachi, Tokyo, Japan) with gallic acid as the standard. The contents of polysaccharide and protein in SNE were determined using the phenol−sulfuric acid method and Bio-Rad protein assay kit, respectively.

**Characterization of Phenolic Compounds of SNE.** Analyses were performed on a Finnigan Surveyor Modular HPLC system (Thermo Electron Co., United States). The chromatographic separation of the compounds was achieved using an analytical column: Luna 3 $\mu$m C18-(2) 150 mm × 2.0 mm and guard column, SecurityGuard C18 (ODS) 4 mm × 3.0 mm i.d. (Phenomenex, Inc., Torrance, CA) at a flow rate of 0.2 mL/min. Mobile phases A and B were water and acetonitrile, respectively, both containing 0.1% formic acid. Gradient elution was conducted as follows: 0−15 min of 5% B, 15−50 min of 5−40% B, and 50−55 min of 40−95% B with a linear gradient, followed by 55−65 min of 95% B isocratic. A photodiode array detector was operated at wavelengths between 220 and 400 nm. The system was coupled to a Finnigan LCQ Advantage MAX ion trap mass spectrometer and operated in electrospray ionization (ESI) mode. Samples of 20 $\mu$L of extracts were directly injected into the column using a Rheodyne (model 7725i) injection valve. The ESI source and negative ionization mode were used with different fragment voltages. Nitrogen was used as the nebulizing and drying gas. The typical operating parameters were as follows: spray needle voltage, 5 kV; ion transfer capillary temperature, 300 °C; nitrogen sheath gas, 40; and auxiliary gas, 5 (arbitrary units). The ion trap contained helium damping gas, which was introduced in accordance with the manufacturer's recommendations. Mass spectra were acquired in a *m*/*z* range of 100−1000, with five microscans and a maximum ion injection time of 200 ms. The SIM analysis was a narrow scan event that monitored the *m*/*z* value of the selected ion, in a range of 1.0 Th centered on the peak for the molecular ion; this function was used in the analysis of molecular ions of the flavonoids for MS/MS in negative ESI modes. The MS/MS fragment spectra were produced using normalized collision energies with an increment of 30% and also with wideband activation "off" (*10*).

**Table 1.** Dry Weight, Polyphenol, Polysaccharide, and Protein Content of Water Extract of SNE

| SNE | % |
|---|---|
| dry weight | 23.13 ± 2.095 |
| polyphenol | 20.35 ± 0.967 |
| polysaccharide | 14.92 ± 1.333 |
| protein | 4.81 ± 0.422 |

**Cell Culture and SNE Treatment.** HepG2, a human liver cancer cell line; WRL-68, a human fetal liver cell line; Chang liver, a human liver cell line; 3T3-L1, mouse embryonic fibroblast; MCF-7, human breast adenocarcinoma; MDA-MB-231, human adenocarcinoma (grade III); and AGS, human gastric adenocarcinoma, were obtained from ATCC (Manassas, VA). HepG2, WRL-68, 3T3-L1, MCF-7, and MDA-MB-231 cells were cultured in Dulbecco's modified Eagle's medium (Life Technologies, Grand Island, NY) supplemented with 10% fetal bovine serum (FBS), 2 mM glutamine, 100 U/mL penicillin, 100 mg/mL streptomycin sulfate, 0.1 mM nonessential amino acid, and 1 mM sodium pyruvate. Chang liver cells were cultured in Basal medium Eagle (Sigma, Steinheim, Germany) supplemented with 10% calf serum, 100 U/mL penicillin, and 100 mg/mL streptomycin sulfate. AGS cells were cultured in 90% Ham's F-12K medium supplemented with 10% FBS. All cell cultures were maintained at 37 °C in a humidified atmosphere of 5% $CO_2$. For SNE treatment, appropriate amounts of stock solution (100 mg/mL in culture medium) of SNE were added to the cultured cells to achieve the indicated concentrations and then incubated for the indicated time periods. In time−course experiments, the cells were treated with SNE of 10, 50, 100, and 500 $\mu$g/mL and 1, 2, and 5 mg/mL for the indicated periods.

**Determination of Cell Viability [3-(4,5-Dimethylthiazol-2-yl)-2,5-diphenyltetrazolium Bromide (MTT) Assay].** To evaluate the cytotoxicity of SNE, the MTT assay was performed to determine the cell viability (*11*). Cells were seeded in 24 well plates at a density of 3.5 × $10^4$ cells/well and treated with SNE at 0−5 mg/mL concentration at 37 °C for 24 and 48 h. In inhibition experiments, cells were pretreated with 2 mM 3-MA. After the exposure, media were removed, and the cells were washed with phoshate-buffered saline (PBS). Thereafter, the medium was changed to the one containing 100 $\mu$L MTT (5 mg/mL)/well for another 4 h incubation. The viable cell number per dish was directly proportional to the production of formazan, which was solubilized in isopropanol, and was measured spectrophotometrically at 563 nm.

**Flow Cytometric Analysis.** Cells synchronized at the $G_0$ phase by serum starvation for 24 h were incubated in fresh medium containing 10% v/v FBS to allow the progression through the cell cycle. At various time periods after relief of the quiescent state, the cells were analyzed for cell cycle distribution by flow cytometry (*12*). After various treatments, HepG2 cells were treated with trypsin and RNase and then stained with propidium iodide (PI). The cell cycle distribution was presented as the number of cells vs the amount of DNA as indicated by the intensity of fluorescence, and the extent of apoptosis was determined by counting cells of DNA content below the Sub-G1 peak.

**Western Blot Analysis.** After the indicated SNE treatment, the medium was removed, and the cells were rinsed with PBS twice. After the addition of 0.1 mL of cold radioimmunoprecipitation assay buffer and protease inhibitors, the cells were scraped followed by a vortex at 0 °C for 10 min. The cell lysate was then subjected to a centrifugation of 10000*g* for 10 min at 4 °C. Resultant protein samples were separated in a 12.5% polyacrylamide gel and transferred onto a nitrocellulose membrane as previously described. The blot was sequentially incubated with 5% nonfat milk in PBS for 1 h to block nonspecific binding, with

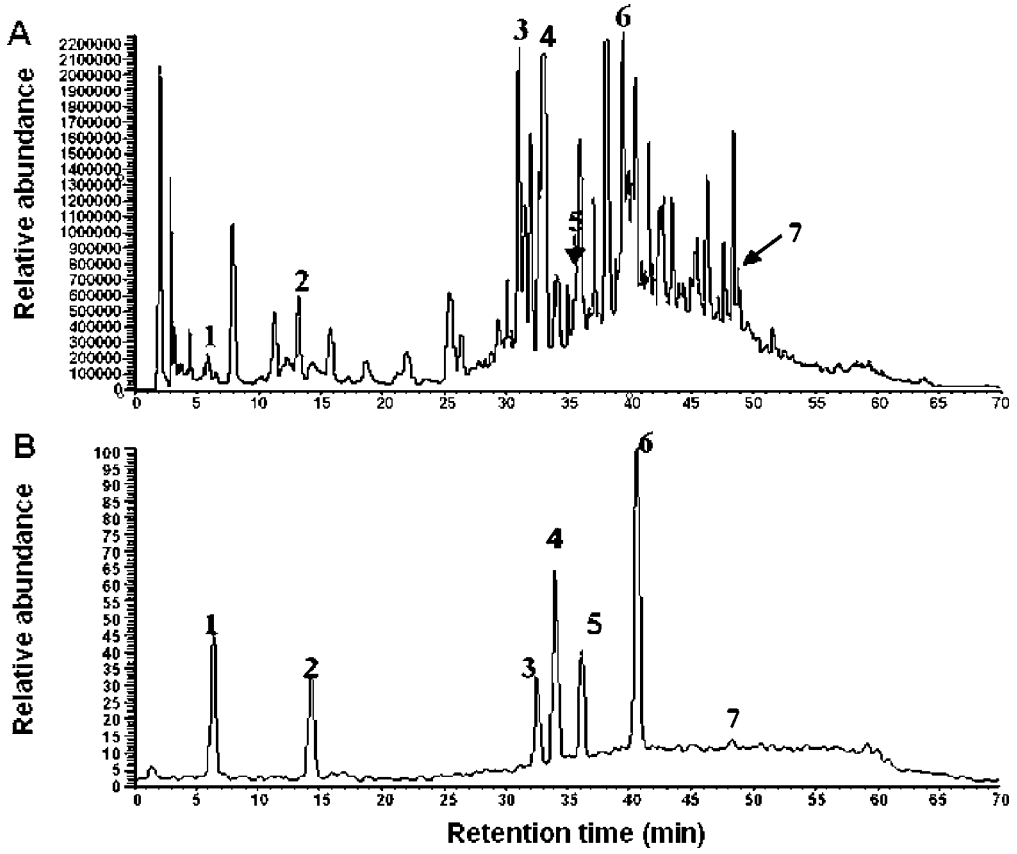


**Figure 1.** (**A**) HPLC/UV chromatogram (278 nm) of the water extract of SNE. Polyphenolic compounds correspond to peaks 1–7 in part **B** are marked. (**B**) Ion chromatograms extracted at *m*/*z* corresponding to the molecular mass of the identified phenolic compounds. Peaks: 1, gallic acid; 2, proto catechuic acid (PCA); 3, catechin; 4, caffeic acid; 5, epicatechin; 6, rutin; and 7, naringenin.

a polyclonal antibody against phospho-JNK, hospho-Akt (Cell Signaling Tech., MA), Bax, cytochrome *c*, caspase 3, Bcl-2 (Senta Cruz, CA), or LC3 (kindly provided by Drs. Yoshimori and Mizushima, National Institute for Basic Biology, Okazaki, Japan) for 2 h and then with an appropriate peroxidase-conjugated secondary antibody (Sigma, St. Louis, MO) for 1 h. All incubations were carried out at 37 °C, and intensive PBS washing was performed between each incubation. After the final PBS wash, the signal was developed by 4-chloro-1-napthol/3,3-*o*-diaminobenzidine, and the relative photographic density was quantitated by scanning the photographic negatives by a gel documentation and analysis system (Alpha Imager 2000, Alpha Innotech Corp., San Leandro, CA).

**Electron Microscopy.** The cells were harvested by trypsinization, washed twice with PBS, and fixed with 2% glutaraldehyde, 4% paraformaldehyde, and 1% tannic acid in 0.1 mol/L cacodylate buffer, pH 7.4, for 25 h at 4 °C. After they were washed with PBS, the cells were stained with osmium−thiocarbohydrazide−osmium. This procedure was carried out by incubating cells in 1% $OsO_4$ in 0.1 mol/L cacodylate buffer, pH 7.4, for 1 h followed by 1% thiocarbohydrazide in $H_2O$ for 15 min and then 1% $OsO_4$ for 15 min. Extensive washing of cells with distilled water was performed between each step. After staining, the cells were dehydrated in a graded series of EtOH to 100% EtOH and then immersed serially with 1:1 hexamethyldisilazane and absolute ethanol and pure hexamethyldisilazane for 5 min each. After air drying from hexamethyldisilazane overnight, the cells were embedded in agarose gel. One micrometer thin sections were cut, and the gels were coated with 500 Å of gold in a JEOL Vacuum sputter coater and viewed in a JEOL T300 electron microscope with scanning attachment (JEOL, Tokyo, Japan) (*13*).

**Detection of Acidic Vesicular Organelles (AVOs) with Acridine Orange Staining.** To detect AVOs in SNE-treated cells, the vital staining with acridine orange was performed as described previously (*14*). The treated tumor cells were stained with acridine orange, which was added at a final concentration of 1 $\mu$g/mL for 15 min. Samples were then examined under a fluorescence microscope. Acridine orange labelled AVO, such as autophagosomes. A typical acridine orange-positive cell exhibited granular distribution of acridine orange in the cytoplasm, indicative of autophagosome formation.

**Statistical Analysis.** Statistical significances were analyzed by one-way analysis of variance (ANOVA) with posthoc Dunnett's test. A $p$ value of $\leq 0.05$ was considered statistically significant (Sigma-Stat 2.0, Jandel Scientific, San Rafael, CA).

## RESULTS

**Composition of SNE.** To establish the composition of SNE from SN, the contents of polyphenol and polysaccharide were assayed, and the concentrations of polyphenolic acids were determined by high-performance liquid chromatography (HPLC). As shown in **Table 1**, the dry weight yield of SNE was 23.125 ± 2.095%, consisting of 20.35 ± 0.967% total polyphenolics using gallic acid as the standard and 14.92 ± 1.333% polysaccharide. Polysaccharide is usually associated with protein as complexes; the result indicated that SNE contained 4.81 ± 0.442% protein. HPLC analysis of the standard polyphenols showed that the retention times of gallic aicd, protocatechuic acid (PCA), catechin, caffeic acid, epicatechin, rutin, and naringenin were 6.2, 13.49, 31.48, 32.84, 35.61, 4.035, and 49.16 min, respectively (**Figure 1** and **Table 2**). The analysis of SNE revealed the presence of gallic acid (2.897%), PCA (1.977%), catechin (2.353%), caffeic acid (1.988%), epicatechin (0.392%), rutin (0.836%), and naringenin (5.106%). The further identities of the seven components were established from recorded mass spectra. The mass spectra of the phenolic acids are listed in **Table 2**. The extract was stored at −20 °C and used in the following studies. In the present study, we have identified the contents of polysaccharides and proteins in SNE and characterized seven phenolic compounds of SNE.

**Table 2.** Characterization of Phenolic Compounds of SNE

| peak no. | retention time (min) | assigned identity | recovery (%) | UV $\lambda_{max}$ (nm) | $[M-H]^-$ *m/z* | LC/ESI-MS$^{2a}$ *m/z* |
|---|---|---|---|---|---|---|
| 1 | 6.20 | gallic acid | 2.897 ± 1.1 | 270, 225 | 168.9 | 125.0 |
| 2 | 13.49 | PCA | 1.977 ± 0.95 | 222, 259 | 153.1 | 108.9 |
| 3 | 31.48 | catechin | 2.353 ± 1.05 | 230, 229 | 289.1 | 245.2, 205.1 |
| 4 | 32.84 | caffeic acid | 1.533 ± 0.63 | 256, 354 | 178.9 | 135.0 |
| 5 | 35.61 | epicatechin | 1.988 ± 0.49 | 230, 279 | 289.0 | 245.1 |
| 6 | 40.35 | rutin | 0.836 ± 0.32 | 256, 354 | 609.2 | 301.1, 343.1 |
| 7 | 49.16 | narigenin | 5.106 ± 2.01 | 231, 288 | 271.1 | 150.9, 177.1 |

[a] $MS^2$ run with 30% collision energy.

**Cytotoxic Effects of SNE on HepG2 Cells.** In this study, we first determined the cytotoxicity of SNE by treating HepG2, WRL-68, and Chang liver cells with SNE at various concentrations for 24 and 48 h followed by MTT assay. The human hepatic cell line WRL-68 has a morphological structure similar to hepatocytes and hepatic primary cultures. Derived from fetal liver, WRL-68 cells secrete α-fetoprotein and albumin, preserve the activity of some characteristic or specific liver enzymes (i.e., alanine aminotransferase, aspartate aminotransferase, γ-glutamyl transpeptidase, and alkaline phosphatase), and exhibit a cytokeratin pattern similar to other hepatic cultures, providing an in vitro model to study the toxic effects of xenobiotics (*15*).

The addition of SNE exerted a cytotoxic effect in a dose- and time-dependent manner (**Figure 2A**,**B**). Following a 24 h incubation with 50 μg/mL SNE in HepG2 cells, the cytotoxicity was around 22.7−27.4% (**Figure 2A**). However, when 100−5000 μg/mL extract was added, a significant increase in cytotoxicity was observed. Furthermore, a time-dependent increase in SNE-induced cytotoxicity was also detected (**Figure 2B**). The strongest potency of SNE on the cytotoxicity of cells was toward HepG2 liver cancer cells. The concentration of SNE on the inhibition of 50% of HepG2 cells viability ($IC_{50}$) was 0.625 mg/mL. However, the $IC_{50}$ values of SNE to the death of Chang liver (human liver cells; $IC_{50}$, 3.2 mg/mL SNE) and WRL-68 (human fetal liver cell; $IC_{50}$, 3.0 mg/mL SNE) were 5.12- and 4.8-fold higher than that of HepG2 cells, indicating that SNE is less cytotoxic to normal cells. As compared to normal liver cells, SNE seems to have a stronger death effect toward liver cancer cells, HepG2. We further determined the cytotoxicity of SNE on other normal cells, 3T3-L1, and cancer cells, MCF-7, MDA-MB-231, and AGS, at various concentrations for 48 h followed by MTT assay. The results indicated that SNE is more cytotoxic to tumor cells.

**SNE-Induced Apoptotic Death of HepG2 Cells.** HepG2 cells treated with 2 and 5 mg/mL SNE for 48 h showed typical apoptotic features: cell shrinkage, membrane blebbing, and apoptotic bodies as observed under inverted microscopy. To further confirm that programmed cell death was involved in the cytotoxic effect of SNE on liver cancer cells, SNE-treated HepG2 cells were subjected to apoptosis assays by PI staining of nuclei as described in the Materials and Methods, and the apoptotic state was quantitated by flow cytometry. The results indicated that after a treatment with high concentration (2 and 5 mg/mL) of SNE for 48 h, an increased proportion of apoptotic cells was observed (**Figure 3A**). The ratio of cells at the hypodiploid phase was increased to 30.01 and 37.88% when HepG2 cells were exposed to 2.0 and 5.0 mg/mL SNE for 48 h, respectively (**Figure 3A**). The results indicated that high doses of SNE induced apoptotic cell death in HepG2 cells.

**Effect of SNE on JNK Phosphorylation and Bax Protein Expression.** JNK plays an important role in apoptotic signaling. In some cell types, JNK regulates the activities of pre-existing

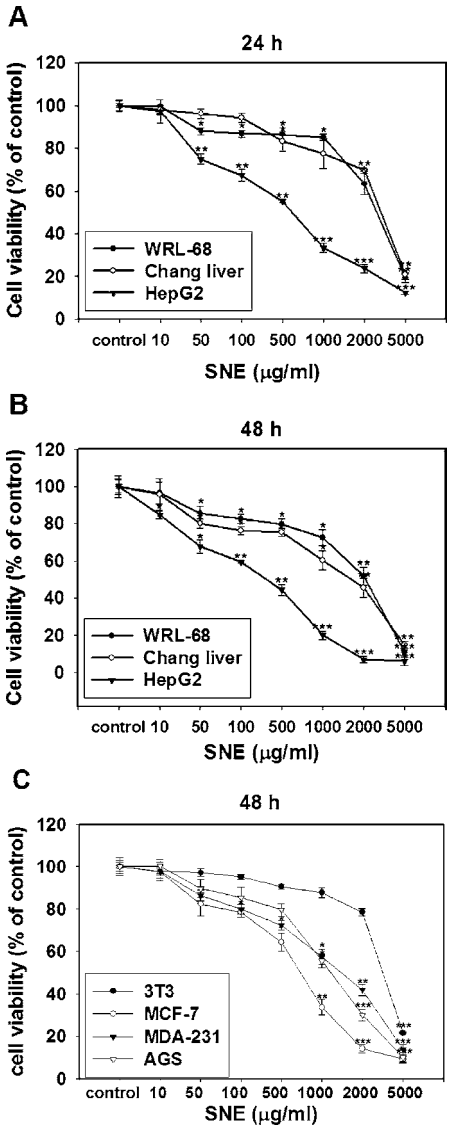


**Figure 2.** Effects of SNE on the viability of tumor cells (HepG2, Chang liver, MCF-7, MDA-231, and AGS cells) and normal cells (WRL-68 and 3T3 cells). Cells were treated with 0, 10, 50, 100, 500, 1000, 2000, or 5000 μg/mL of SNE for 24 and 48 h before they were subjected to a MTT assay for cell viability. The data were expressed as a percentage of the control (dose 0) and presented as means ± SD from three independent experiments. Results were statistically analyzed with Student's *t*-test (*$P < 0.05$, **$P < 0.01$, and ***$P < 0.001$).

Bcl-2 family proteins that mediate mitochondrial release of cytochrome *c*, resulting in caspase activation (*16*). We investigated whether the SNE-induced apoptosis was modulated by the activation of JNK. The results showed that the cellular level of phospho-JNK was significantly increased to 2.65- and 2.81-

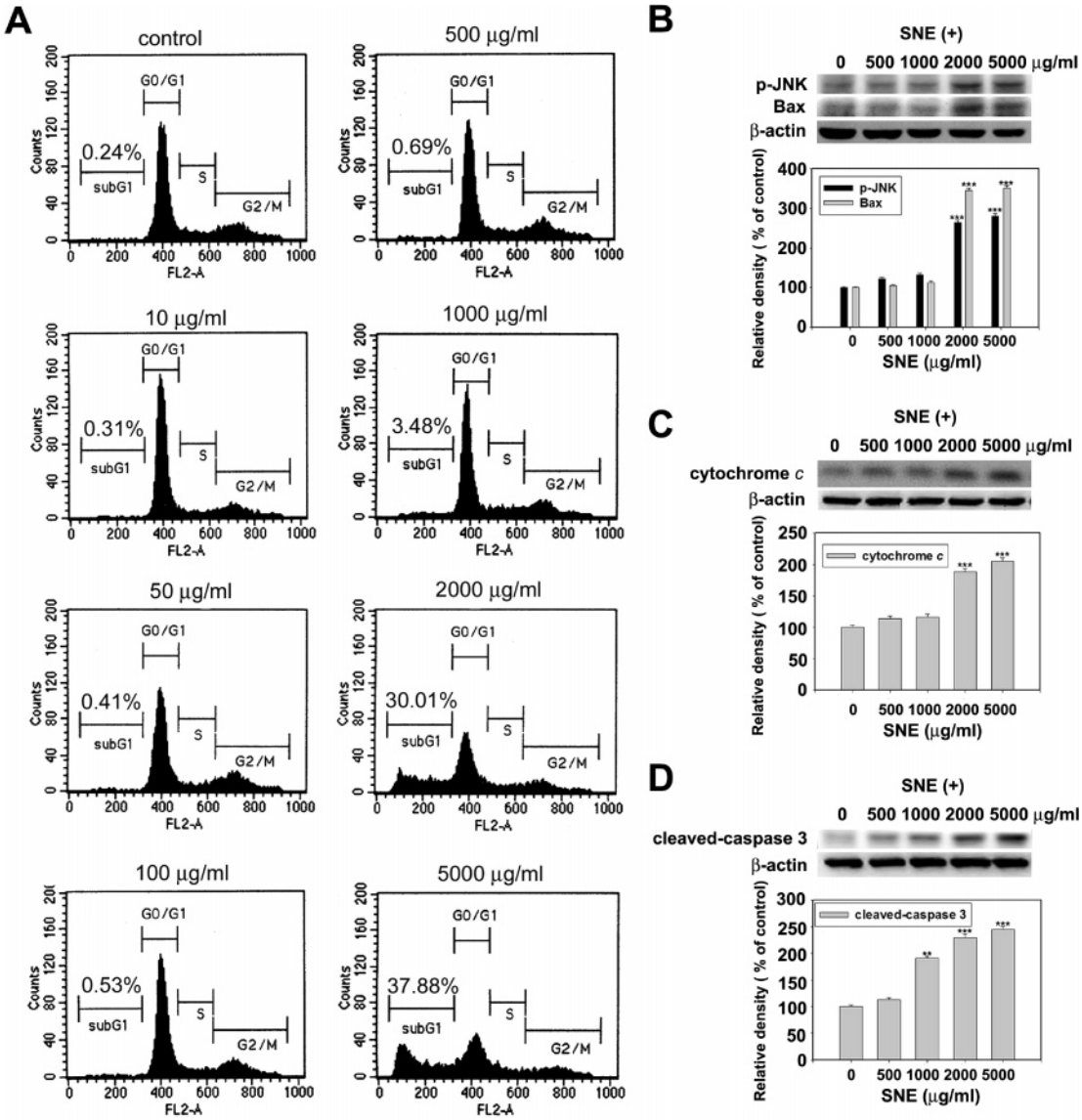


**Figure 3.** Apoptosis effects of SNE on HepG2 cells. (**A**) HepG2 cells were treated with 0, 10, 50, 100, 500, 1000, 2000, or 5000 $\mu$g/mL of SNE for 48 h and subjected to flow cytometric analysis after PI staining. The figure shows a representative staining profile for 8000 cells per experiment. Sub G1 was defined as apoptotic cells. The figure is representative of three independent experiments. (**B**–**D**) Effects of SNE on the expression of apoptotic protein. HepG2 cells were treated with SNE at a concentration of 0, 500, 1000, 2000, and 5000 $\mu$g/mL for 48 h and then subjected to Western blotting to analyze (**B**) p-JNK and Bax, (**C**) cytochrome *c*, and (**D**) cleaved caspase 3 expression as described in the Materials and Methods. The levels of these proteins were subsequently quantitated by densitometric analysis; that of the control was 100%. Data were presented as means ± SD from three independent experiments. Results were statistically evaluated by using one-way ANOVA with posthoc Dunnett's test (**$P$ < 0.01 and ***$P$ < 0.001).

fold ($P$ < 0.001) of the control level under a treatment of 2 and 5 mg/mL SNE, respectively (**Figure 3B**). Investigations of the bcl-2 gene family that encodes integral membrane proteins have shown a complex network regulating apoptosis in multiple biological systems (*17*). We examined the cellular levels of Bax after the treatment of SNE for 48 h in HepG2 cells. The expressions of Bax were significantly induced by the treatment of 2 and 5 mg/mL of SNE to 3.45- and 3.52-fold ($P$ < 0.001), respectively (**Figure 3B**). SNE induced apoptotic cell death in HepG2 cells, as evidenced by an increase in the expression of p-JNK and Bax.

**Effect of SNE on Cytochrome *c* Release and Caspase 3 Cleavage.** Because cytochrome *c* is reported to be involved in the activation of the caspase that executes apoptosis (*18*), we examined the level of cytochrome *c* in the cytosol by Western blot analysis. The results showed that the amount of cytosolic cytochrome *c* increased 1.88- and 2.05-fold ($P$ < 0.001) in the 2 and 5 mg/mL SNE-treated HepG2 cells (**Figure 3C**). Caspase 3 is a cytosolic protein that exists normally as an inactive precursor with higher molecular masses (32 kDa) that is cleaved proteolytically into low molecular masses (20 kDa) when the cell undergoes apoptosis (*19*). In this study, there was an increase in the activation of caspase 3 to 1.91-, 2.3-, and 2.45-fold (**$P$ < 0.01 and ***$P$ < 0.001) of control level in response to 1, 2, and 5 mg/mL SNE treatment, respectively (**Figure 3D**). The results indicated that addition of SNE exerted an apoptotic effect in HepG2 cells by increases in the mitochondrial release of cytochrome *c* and activation of caspase 3.

**Low Concentration of SNE-Induced Autophagic Cell Death in HepG2 Cells.** The flow cytometric data (**Figure 3A**) showed that there was only a very small portion (<4%) of HepG2 cells that displayed a typical morphology of apoptosis when the cells were exposed to low concentrations (50−1000 $\mu$g/mL) of SNE. At the same circumstances, the survival rates

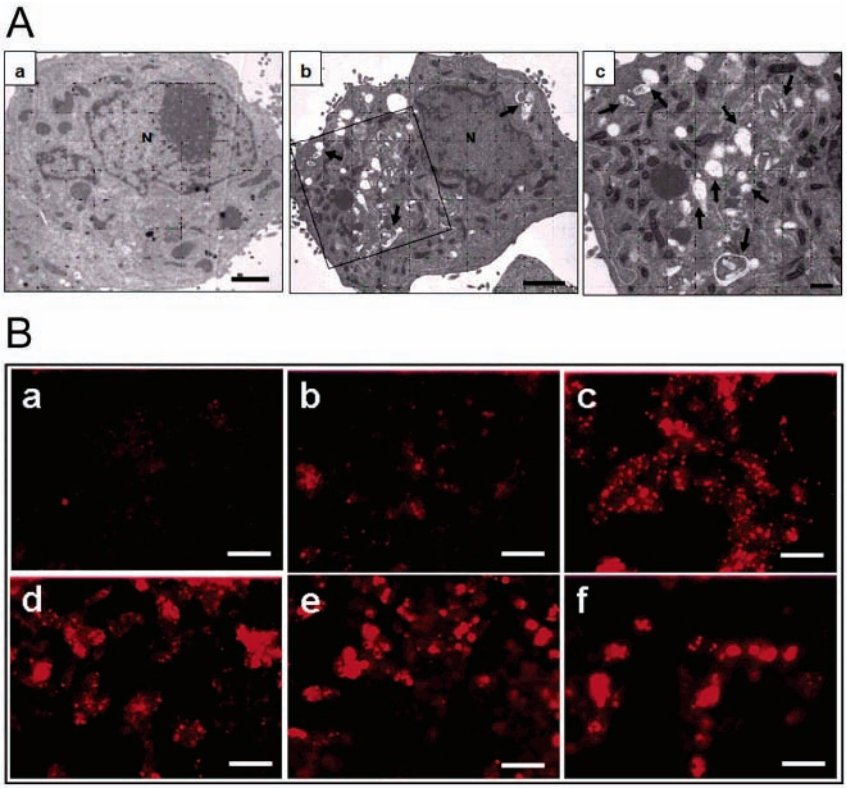


**Figure 4.** SNE-induced autophagic death in HepG2 cells. (**A**) Electron micrographs showing the ultrastructure of HepG2 cells treated with SNE (100 $\mu$g/mL) for 48 h. (a) Control; very few autophagic vacuoles were observed in un-treated HepG2 cells. (b) SNE-treated HepG2 cells. Numerous autophagic vacuoles (arrows) were observed. Bars a and b, 2 $\mu$m; c, an ultrastructure of SNE-treated HepG2 cells at high magnification containing numerous autophagic vacuoles (arrows). Bar c, 3 $\mu$m. (**B**) After addition of SNE for 48 h, acridine orange stain of HepG2 cells showed AVOs formation in a dose-dependent manner. Key: a, 0; b, 10; c, 50; d, 100; e, 500; and f, 1000 $\mu$g/mL. Bars, 50 $\mu$m.

were down to 67.7 and 20% for 50 and 1000 $\mu$g/mL, respectively (**Figure 2B**). These observations indicated that some other death mechanism was initiated in HepG2 cells in response to the treatment of low concentrations (50−1000 $\mu$g/mL) of SNE.

Electron microscopic characterization, which has been the gold standard for determining the mode of cell death, was next used to distinguish between apoptosis, necrosis, and nonapoptotic programmed cell death. Nonapoptotic programmed cell death is principally attributed to autophagy (type II programmed cell death). Autophagy is series of biochemical steps through which eukaryotic cells commit suicide by degrading their own cytoplasm and organelles through a process in which these components are engulfed and then digested in double membrane-bound vacuoles called autophagosomes (*20*). Transmission electron microscopic analysis of HepG2 cells without SNE treatment revealed normal nuclear and mitochondrial morphology (**Figure 4A**, a). On the other hand, HepG2 cells treated with 100 $\mu$g/mL SNE for 48 h revealed extensive vacuolization, formation of membranous whorls (also called myelin figures), and depletion of organelles, which are hallmarks of autophagy (**Figure 4A**, b,c). Cells undergoing autophagic cell death retained an intact nuclear membrane, without chromatin condensation. Initiation of autophagy was associated with an accumulation of lipid droplets in cytoplasm (fatty change of hepatocytes) (**Figure 4A**, b). This event is due to a decline in protein synthesis (vide infra), which blocks the utilization of lipids for lipid−protein conjugation and is typical of hepatocytes undergoing cellular stress (*21*).

Autophagy is characterized by AVO formation, which is detected and measured by vital staining of acridine orange. Acridine orange moves freely to cross biological membranes and accumulates in acidic compartment, where it is seen as fluorescence bright red (*22*). As shown in **Figure 4B**, b−f, vital staining of HepG2 cells with acridine orange showed the accumulation of AVO in the cytoplasm of cells exposed to 10−1000 $\mu$g/mL of SNE. In contrast, there were relatively few AVOs in the cytoplasm of control cells (**Figure 4B**, a). These data indicated that HepG2 cells treated with a low concentration of SNE revealed morphology and ultrastructural changes of autophagocytic death and increased levels of autophagic vacuoles.

**Involvement of LC3 in SNE-Induced Autophagy.** LC3 is localized in autophagosome membranes during amino acid starvation-induced autophagy (*23*). A recent investigation showed that there are two forms of LC3 proteins in cells: LC3-I and LC3-II (*22*). LC3-I is the cytoplasmic form of LC3 and is processed into LC3-II, which is associated with the autophagosome membrane. Therefore, the amount of LC3-II is correlated with the extent of autophagosome formation. Using the immunoblotting analysis with anti-LC3 antibody, we examined the expressions of LC3-I (18 kDa) and LC3-II (16 kDa) in HepG2 cells treated with SNE. As shown in **Figure 5A**, the level of total LC3 (LC3-I and LC3-II proteins) increased in HepG2 cells 24 h after exposure to SNE. Moreover, a marked increase in LC3-II protein was also detected in these cells. These results indicate that SNE stimulated not only the accumulation of LC3 protein but also the conversion of a fraction of LC3-I into LC3-II. LC3 was involved in the SNE-induced autophagy in HepG2 cells.

**Effect of SNE on Bcl-2 Expression and Akt Phosphorylation.** Autophagy is a multistep process, and various signaling pathways have been implicated in its up- or down-regulation. Bcl-2 has also been shown to regulate autophagy in cancer cells.

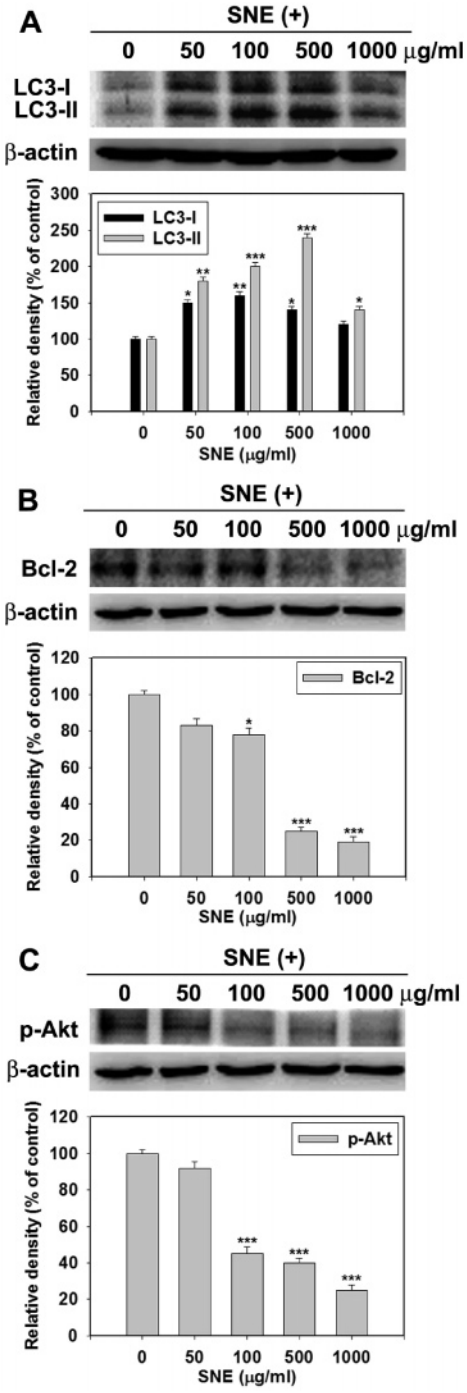


**Figure 5.** Involvement of LC3, Bcl-2, and p-Akt in SNE-induced autophagy in HepG2 cells. HepG2 cells were treated with SNE at a concentration of 0, 50, 100, 500, or 1000 $\mu$g/mL for 12 h and then subjected to Western blotting to analyze (**A**) LC3, (**B**) Bcl-2, and (**C**) p-Akt expression as described in the Materials and Methods. The levels of these proteins were subsequently quantitated by densitometric analysis; that of the control was 100%. Data were presented as means ± SD from three independent experiments. Results were statistically evaluated by using one-way ANOVA with posthoc Dunnett's test (*$P$ < 0.05, **$P$ < 0.01, and ***$P$ < 0.001).

Down-regulation of Bcl-2 using antisense technology triggered autophagy, but not apoptosis, in HL60 human leukemic cells (*24*). We investigated whether the SNE-induced autophagy was modulated by Bcl-2. The results showed that the cellular level of Bcl-2 was significantly decreased to 80, 25, and 18% of that of control in the cells exposed to 100, 500, and 1000 $\mu$g/mL of SNE treatment, respectively (**Figure 5B**). Furthermore, Akt is

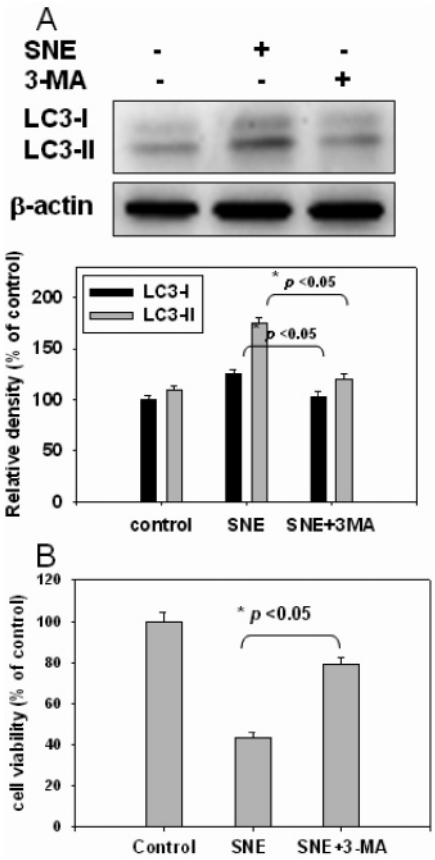


**Figure 6.** 3-MA partially blocked the SNE-induced LC3 expression and cell death. HepG2 cells were pretreated with 2 mM 3-MA for 1 h before SNE (0.5 mg/mL) treatment. (**A**) 3-MA inhibited LC3-I and LC3-II conversion, and (**B**) 3-MA decrease SNE-induced cell death. The levels of these proteins were subsequently quantitated by densitometric analysis; that of the control was 100%. Data were presented as means ± SD from three independent experiments. Results were statistically evaluated by one-way ANOVA with posthoc Dunnett's test (*$P$ < 0.05).

a serine−threonine kinase, located downstream of class I PI3K, that activates the kinase mTOR, leading to suppression of autophagy. We examined the level of phospho-Akt in the cytosol by Western blot analysis. The results showed that the amount of phospho-Akt decreased to 45, 40, and 25% of control in the cells exposed to 100, 500, and 1000 $\mu$g/mL of SNE treatment, respectively ($P$ < 0.001) (**Figure 5C**). These results indicate that Bcl-2 and Akt were involved in the SNE-induced autophagy.

**3-MA Partially Blocked the SNE-Induced LC3-II Conversion and Cell Death.** To confirm the contribution of autophage in the SNE-induced cell death, we used the autophagy inhibitor 3-MA, a class III-PI3K inhibitor, to inhibit the autophagy. The MTT assays show that 2 mM 3-MA could partially prevent SNE-induced cell death (**Figure 6B**). The induction of LC3-I and LC3-II expression was also inhibited by 3-MA (**Figure 6A**). On the basis of these data, we concluded that SNE could induce HepG2 cells to undergo autophagic cell death.

## DISCUSSION

SN is a common herb that grows wildly and abundantly in open fields. It has been used in traditional folk medicine because of its diuretic and antipyretic effects. More specifically, it has been used to cure inflammation, edema, mastitis, and hepatic cancer for a long time in Oriental medicine (*25*). The phytochemical studies revealed the presence of an alkaloid called

solamargine, nigrum I, nigrum II, and a glycoside named solasodine (*7*). It has also been shown that SN contains many polyphenolic compounds, mainly flavonoids and steroids. Our results showed that SNE consists of 14.92% polysaccharides, 4.81% protein, and 20.35% total polyphenols, such as gallic acid (2.897%), PCA (1.977%), catechin (2.353%), caffeic acid (1.988%), epicatechin (0.392%), rutin (0.836%), naringenin (5.106%), and unknown polyphenols (**Tables 1** and **2** and **Figure 1**). The antioxidant and antitumor activity of these extracts have been suggested to be due to the presence of polysaccharides and polyphenolic constituents. Nevertheless, there is little conclusive evidence demonstrating the effectiveness of SN on treating already existing 50−1000 $\mu$g/mL tumors or malignancies animals.

Our results demonstrated a significant cytotoxic effect of SNE on HepG2 cells that was mediated via two mechanisms depending on the exposed concentrations. When HepG2 cells were treated with a high concentration (2 and 5 mg/mL) of SNE, the cells underwent apoptotic cell death as evidenced by increases in sub-G1 cells and cellular levels of phospho-JNK, Bax, cytosolic cytochrome *c*, and cleaved-caspase 3. The exposure of a low concentration (50−1000 $\mu$g/mL) of SNE did not result in apoptosis, but rather, our results point to autophagocytosis (autophagy of type II programmed cell death) as the main mode of death under such conditions.

Autophagy is a physiological mechanism that involves the sequestration of cytoplasm and intracellular organelles into membrane vacuoles and results in their eventual enzymatic degradation (*20*). In response to appropriate stimulation, depolarized mitochondria are known to move into autophagic vacuoles. Thus, mitochondrial dysfunction may be a point of overlap between apoptotic and autophagocytic processes (*26*). The fusion of the edges of the membrane sac forms a closed double-membrane structure, the so-called autophagosome. Finally, the autophagosome fuses with a lysosome to become the autolysosome within which lysosomal hydrolases degrade the sequestered cellular constituents. HepG2 cells treated with 50−1000 $\mu$g/mL of SNE demonstrated an ultrastructural appearance consistent with the characteristics of autophagy under electron microscopic observation. Furthermore, SNE-treated cells were able to be stained with acridine orange, a specific marker for autophagic vacuoles (*22*). Confirmatory experiments were performed with anti-LC3 antibody showing that SNE stimulated not only the expression of LC3 protein but also the conversion of a fraction of LC3-I into LC3-II. We also demonstrated that 3-MA could block the SNE-induced LC3-II conversion and cell death. Furthermore, the levels of Bcl-2 and Akt that have been implicated in down-regulation of autophagy were decreased upon SNE treatment, confirming the involvement of Bcl-2 and Akt in the SNE-induced autophagy (*24*).

Nonapoptotic cell death is mainly attributed to autophagy, which is considered to be an alternative way to kill tumor cells when the cells are chemoresistant on the basis of ineffective apoptosis. A number of studies have reported that autophagy is activated in cancer cells in response to various anticancer therapies, such as tamoxifen in breast cancer cells (*27*), temozolomide (TMZ, a DNA alkylating agent), and arsenic trioxide in malignant glioma cells (*28*). As for natural products, resveratrol, a phytoalexin that is present in grape nuts and red wine, induced autophagy in ovarian cancer cells (*29*), and soybean B group triterpenoid saponins caused autophagy in colon cancer cells (*30*). The results of present study add SNE to the list of natural products that possess autophagic effects in addition to its apoptotic effect. We have demonstrated that the cytotoxic effects after exposure to a high concentration (2 and 5 mg/mL) of SNE is caused by apoptosis and a low concentration of SNE is caused by autophagy. However, the molecular basis for the different effect responding to high and low concentrations of SNE needs further investigation. There might be a cross-talk between the pathways of apoptosis and autophagy.

In summary, we have identified two distinct antineoplastic activities of SNE in liver cancer cells, the ability to induce apoptosis and autophagocytosis. This response and its ability to kill these cells hint at the possibility that this agent may be useful as an adjuvant therapy to treat liver tumors. These findings pave the way for additional experiments to consider the molecular basis for this response and studies to determine whether adequate concentrations of bioactive SNE can be attained to treat liver tumors.

## ACKNOWLEDGMENT

We thank Dr. Tamotsu Yoshimori for his kind gift of reagents.

## LITERATURE CITED

(1) Tong, W. M.; Lee, M. K.; Galendo, D.; Wang, Z. Q.; Sabapathy, K. Aflatoxin-B exposure does not lead to p53 mutations but results in enhanced liver cancer of Hupki (human p53 knock-in) mice. *Int. J. Cancer* **2006**, *119*, 745−749.

(2) Son, Y. O.; Kim, J.; Lim, J. C.; Chung, Y.; Chung, G. H.; Lee, J. C. Ripe fruit of *Solanum nigrum* L. inhibits cell growth and induces apoptosis in MCF-7 cells. *Food Chem. Toxicol.* **2003**, *41*, 1421−1428.

(3) Sultana, S.; Perwaiz, S.; Iqbal, M.; Athar, M. Crude extracts of hepatoprotective plants, *Solanum nigrum* and *Cichorium intybus* inhibit free radical-mediated DNA damage. *J. Ethnopharmacol.* **1995**, *45*, 189−192.

(4) Prashanth Kumar, V.; Shashidhara, S.; Kumar, M. M.; Sridhara, B. Y. Cytoprotective role of *Solanum nigrum* against gentamicin-induced kidney cell (Vero cells) damage in vitro. *Fitoterapia* **2001**, *72*, 481−486.

(5) Yen, G. C.; Chen, H. Y.; Peng, H. H. Evaluation of the cytotoxicity, mutagenicity and antimutagenicity of emerging edible plants. *Food Chem. Toxicol.* **2001**, *39*, 1045−1053.

(6) Lee, S. J.; Oh, P. S.; Ko, J. H.; Lim, K.; Lim, K. T. A 150-kDa glycoprotein isolated from *Solanum nigrum* L. has cytotoxic and apoptotic effects by inhibiting the effects of protein kinase C alpha, nuclear factor-kappa B and inducible nitric oxide in HCT-116 cells. *Cancer Chemother. Pharmacol.* **2004**, *54*, 562−572.

(7) Raju, K.; Anbuganapathi, G.; Gokulakrishnan, V.; Rajkapoor, B.; Jayakar, B.; Manian, S. Effect of dried fruits of *Solanum nigrum* Linn. against $CCl_4$-induced hepatic damage in rats. *Biol. Pharm. Bull.* **2003**, *26*, 1618−1619.

(8) Ikeda, T.; Tsumagari, H.; Nohara, T. Steroidal oligoglycosides from *Solanum nigrum*. *Chem. Pharm. Bull. (Tokyo)* **2000**, *48*, 1062−1064.

(9) Lakenbrink, C.; Lapczynski, S.; Maiwald, B.; Engelhardt, U. H. Flavonoids and other polyphenols in consumer brews of tea and other caffeinated beverages. *J. Agric. Food Chem.* **2000**, *48*, 2848−2852.

(10) La Torre, G. L.; Saitta, M.; Vilasi, F.; Pellicanò, T.; Dugo, G. Direct determination of phenolic compounds in Sicilian wines by liquid chromatography with PDA and MS detection. *Food Chem.* **2006**, *94*, 640−650.

(11) Mosmann, T. Rapid colorimetric assay for cellular growth and survival: Application to proliferation and cytotoxicity assays. *J. Immunol. Methods* **1983**, *65*, 55−63.

(12) Sherwood, S. W.; Schimke, R. T. Cell cycle analysis of apoptosis using flow cytometry. *Methods Cell Biol.* **1995**, *46*, 77−97.

(13) Jiang, S. T.; Liao, K. K.; Liao, M. C.; Tang, M. J. Age effect of type I collagen on morphogenesis of Mardin-Darby canine kidney cells. *Kidney Int.* **2000**, *57*, 1539−1548.

(14) Kanzawa, T.; Kondo, Y.; Ito, H.; Kondo, S.; Germano, I. Induction of autophagic cell death in malignant glioma cells by arsenic trioxide. *Cancer Res.* **2003**, *63*, 2103−2108.
(15) Gutierrez-Ruiz, M. C.; Bucio, L.; Souza, V.; Gomez, J. J.; Campos, C.; Carabez, A. Expression of some hepatocyte-like functional properties of WRL-68 cells in culture. *In Vitro Cell Dev. Biol. Anim.* **1994**, *30*, 366−371.
(16) Tournier, C.; Hess, P.; Yang, D. D.; Xu, J.; Turner, T. K.; Nimnual, A.; Bar-Sagi, D.; Jones, S. N.; Flavell, R. A.; Davis, R. J. Requirement of JNK for stress-induced activation of the cytochrome *c*-mediated death pathway. *Science* **2000**, *288*, 870−874.
(17) Danial, N. N.; Korsmeyer, S. J. Cell death: Critical control points. *Cell* **2004**, *116*, 205−219.
(18) Yang, J.; Liu, X.; Bhalla, K.; Kim, C. N.; Ibrado, A. M.; Cai, J.; Peng, T. I.; Jones, D. P.; Wang, X. Prevention of apoptosis by Bcl-2: Release of cytochrome c from mitochondria blocked. *Science* **1997**, *275*, 1129−1132.
(19) Solary, E.; Plenchette, S.; Sordet, O.; Rebe, C.; Ducoroy, P.; Filomenko, R.; Bruey, J. M.; Droin, N.; Corcos, L. Modulation of apoptotic pathways triggered by cytotoxic agents. *Therapie* **2001**, *56*, 511−518.
(20) Reggiori, F.; Klionsky, D. J. Autophagy in the eukaryotic cell. *Eukaryotic Cell* **2002**, *1*, 11−21.
(21) Martinet, W.; DeMeyer, G. R.; Andries, L.; Herman, A. G.; Kockx, M. M. In situ detection of starvation-induced autophagy. *J. Histochem. Cytochem.* **2006**, *54*, 85−96.
(22) Stankiewicz, M.; Jonas, W.; Hadas, E.; Cabaj, W.; Douch, P. G. Supravital staining of eosinophils. *Int. J. Parasitol.* **1996**, *26*, 445−446.
(23) Mizushima, N.; Yamamoto, A.; Hatano, M.; Kobayashi, Y.; Kabeya, Y.; Suzuki, K.; Tokuhisa, T.; Ohsumi, Y.; Yoshimori, T. Dissection of autophagosome formation using Apg5-deficient mouse embryonic stem cells. *J. Cell Biol.* **2001**, *152*, 657−668.
(24) Kondo, Y.; Kanzawa, T.; Sawaya, R.; Kondo, S. The role of autophagy in cancer development and response to therapy. *Nat. Rev. Cancer* **2005**, *5*, 726−734.
(25) Heo, K. S.; Lee, S. J.; Ko, J. H.; Lim, K.; Lim, K. T. Glycoprotein isolated from *Solanum nigrum* L. inhibits the DNA-binding activities of NF-kappaB and AP-1, and increases the production of nitric oxide in TPA-stimulated MCF-7 cells. *Toxicol. in Vitro* **2004**, *18*, 755−763.
(26) Ogier-Denis, E.; Codogno, P. Autophagy: A barrier or an adaptive response to cancer. *Biochim. Biophys. Acta* **2003**, *1603*, 113−128.
(27) Scarlatti, F.; Bauvy, C.; Ventruti, A.; Sala, G.; Cluzeaud, F.; Vandewalle, A.; Ghidoni, R.; Codogno, P. Ceramide-mediated macroautophagy involves inhibition of protein kinase B and up-regulation of beclin 1. *J. Biol. Chem.* **2004**, *279*, 18384−18391.
(28) Kanzawa, T.; Germano, I. M.; Komata, T.; Ito, H.; Kondo, Y.; Kondo, S. Role of autophagy in temozolomide-induced cytotoxicity for malignant glioma cells. *Cell Death Differ.* **2004**, *11*, 448−457.
(29) Opipari, A. W., Jr.; Tan, L.; Boitano, A. E.; Sorenson, D. R.; Aurora, A.; Liu, J. R. Resveratrol-induced autophagocytosis in ovarian cancer cells. *Cancer Res.* **2004**, *64*, 696−703.
(30) Ellington, A. A.; Berhow, M. A.; Singletary, K. W. Inhibition of Akt signaling and enhanced ERK1/2 activity are involved in induction of macroautophagy by triterpenoid B-group soyasaponins in colon cancer cells. *Carcinogenesis* **2006**, *27*, 298−306.

**Received for review August 21, 2006. Revised manuscript received February 27, 2007. Accepted February 28, 2007. This work was supported by grants from the National Science Council of Taiwan (NSC 94-2320-B-040-040 and NSC95-2321-B-040-001).**

JF062406M